Arabian Journal of Chemistry (2020) **13**, 6425–6436

King Saud University

**Arabian Journal of Chemistry**

www.ksu.edu.sa
www.sciencedirect.com

ORIGINAL ARTICLE

# *Piper longum* catkin extract mediated synthesis of Ag, Cu, and Ni nanoparticles and their applications as biological and environmental remediation agents

**Nargis Jamila [a,*], Naeem Khan [b,**], Amina Bibi [a], Adnan Haider [c], Sadiq Noor Khan [d], Amir Atlas [b], Umar Nishan [b], Aaliya Minhaz [a], Fatima Javed [a], Ahtaram Bibi [b]**

[a] *Department of Chemistry, Shaheed Benazir Bhutto Women University, Peshawar 25000, Khyber Pakhtunkhwa, Pakistan*
[b] *Department of Chemistry, Kohat University of Science and Technology, Kohat 26000, Khyber Pakhtunkhwa, Pakistan*
[c] *Department of Biological Sciences, National University of Medical Sciences, Rawalpindi, Punjab, Pakistan*
[d] *Department of Medical Lab Technology, University of Haripur, Haripur 22060, Khyber Pakhtunkhwa, Pakistan*

Received 28 February 2020; accepted 4 June 2020
Available online 17 June 2020

**KEYWORDS**

*P. longum*;
Elemental content;
Nickel nanoparticles;
Inductively coupled plasma-optical emission spectroscopy;
Atomic force microscopy;
Anticancer

**Abstract** *Piper longum* (long pepper) in dried form is used in several traditional medicines and as a spice. The present study highlights nutritional and toxic elements content, synthesis, and characterization of silver, copper oxide, and nickel nanoparticles using *P. longum* catkin extract. The study also determined anticancer, antioxidant, antimicrobial, and redox catalytic activities of the synthesized NPs. The *P. longum* extract mediated nanoparticles (PLNPs) synthesized at different pH and ratios were characterized by UV–Vis (ultra-violet-visible), FT-IR (Fourier-Transform infrared), and scanning electron and atomic force microscopic (SEM, AFM) techniques. Elemental content of *P. longum* catkin determined by inductively coupled plasma-optical emission spectroscopy (ICP-OES) and ICP-mass spectrometry (ICP-MS) indicated appreciable concentrations of nutritional elements, and well below permissible ranges of toxic elements. Well-defined and stable silver nanoparticles (PLAgNPs) were formed in 1:4 to 1:6 ratios, while copper oxide and nickel NPs (PLCuONPs and PLNiNPs) were found prominent in 1:6 ratio. In determining the effect of pH on synthesized PLNPs, sharp intense absorption peaks were obtained under slightly neutral to highly basic conditions (pH 6 to 13) for PLAgNPs, whereas for PLCuONPs and PLNiNPs, pH 7–8 was optimum. In biological activities, PLNPs exhibited significant anticancer efficacy against DU-145 (prostate cancer) cell line in the range from 92.7% (PLCuONPs) to 100% (PLAgNPs,

* Corresponding author at: Department of Chemistry, Shaheed Benazir Bhutto Women University, Peshawar, Khyber Pakhtunkhwa, Pakistan.
** Corresponding author at: Department of Chemistry, Kohat University of Science and Technology, Kohat, Khyber Pakhtunkhwa, Pakistan.
E-mail addresses: nargisjamila@sbbwu.edu.pk (N. Jamila), nkhan812@gmail.com (N. Khan).
Peer review under responsibility of King Saud University.

Production and hosting by Elsevier

https://doi.org/10.1016/j.arabjc.2020.06.001

PLNiNPs). Fuurthermore, the sythesized NPs exhibited significant antioxidant, antimicrobial, and redox catalytic properties. This study concluded the promising nutritional, biological and environmental remediation applications, and hence, further exploration of the synthesized NPs in biological and clinical applications is currently under investigation.



## 1. Introduction

*Piper* species (Piperaceae), which are widely distributed in Pakistan, India, South Asia, and Australia, have various economic and medicinal values in the drugs as well as food markets. *Piper longum (P. longum)* commonly known as long pepper is used as a spice and traditional medicine to treat digestion problems, diarrhea, asthma, bronchial troubles, sleeping disorders, hemorrhoids, nasal congestion, snake bite, tumors, menstrual problems, and pregnancy (Salehi et al. 2019). It is a rich source of organic constituents including volatile oil, carbohydrates, proteins, alkaloids, sapo-nins, tannins, and mineral nutrients such as K, Mg, Na, Zn, Mn, and Co required for sound human health, metabolic processes, proper growth, and lipid metabolism (Hwang et al., 2016). *P. longum* has also been reported to possess anticancer, antioxidant, hepatoprotective, antimicrobial, antidysenteric, anti–inflammatory, antiplatelet, and anti–obesity properties (Scott et al., 2008; Kumar et al. 2009; Reddy & Zhang, 2013).

Plants can accumulate inorganic toxic metals such as As, Cd, Hg, and Pb in their edible and nonedible parts, which may pose serious health risks upon consumption. In the developing world such as Pakistan, unlike the pharmaceutical products, there are no specific guidelines for toxic contaminants in medicinal herbs and nutraceuticals. Hence, there is a lack of toxic metals assessment of medicinal herbs consumed in Pakistan. However, to ensure the consumers health, there is a great need to assess their content in the consuming herbs. Hence, the current study determines the content of Al, Ca, Fe, K, Mg, Na, P, S, Ni, Cu, Rb, Sr, Zn, V, Cr, Co, Se, Li, Be, Ga, Cs, Ba, As, Cd, In, Tl, Pb, and U in *P. longum* catkin by inductively coupled plasma-optical emission spectroscopy (ICP-OES) and inductively coupled plasma-mass spectroscopy (ICP-MS) techniques.

Plants and herbs due to the presence of enzymes, proteins, amino acids, polysaccharides, polyphenols, and flavonoids, have been used for the synthesis of metal nanoparticles, which play key role in health care, drug delivery, and medicine (Reddy & Zhang, 2013; Dhand et al. 2015; Rajan et al. 2015; Eleftheriadou et al. 2017; Méndez-Albores et al. 2017; Ovais et al. 2018; Silva-Ichante et al. 2018; Tripathi et al. 2019). Previously, several researchers have synthesized metal nanoparticles (MNPs) utilizing *P. longum* extract (Jacob et al. 2012; Mallikarjuna et al. 2013; Reddy et al. 2014; Nakkala et al. 2016; Nasrollahzadeh et al. 2015; Jayapriya et al. 2019; Yadav et al. 2019). However, the current study highlights a detailed synthesis of *P. longum* catkin silver (PLAgNPs), copper oxide (PLCuONPs), and nickel nanoparticles (PLNiNPs) using a wide range of ratios (1:1 to 1:10), and different conditions (stirring, heating, incubation and sunlight, pH). The synthesized NPs were characterized by UV–Vis (ultraviolet-visible), FT-IR (Fourier-Transform infrared), scanning electron microscopy (SEM), and atomic force microscopy (AFM) techniques. The synthesized NPs were further assayed for anticancer potential against DU-145 (prostate cancer) cell line, antioxidant activity (DPPH and ABTS radical scavenging), and antimicrobial capabilities against *Staphylococcus aureus*, *Pseudomonas aeruginosa*, *Bacillus subtilis*, *Escherichia coli*, *Candida albicans*, *Candida krusei*, *Aspergillus flavus*, and *Trichophyton mentagrophytes* strains.

MNPs have been previously used for t due to their greater effeciency as compared to chemical degration by $NaBH_4$ he reduction of dyes/industrial contaminants (Khan et al., 2016, 2018, 2019; Ali et al., 2017; Bello et al., 2017; Anwar et al., 2018; Singh et al., 2018). The current study reports the catalytic properties of the synthesized NPs for the reduction of dyes including methylene blue (MB), Congo red (CR), and food colors; bright red (BR), zarda yellow (ZY), and deep green (DG) with PLNPs.

## 2. Materials and methods

### 2.1. Samples collection

The dried catkin of *P. longum* were procured in triplicates (15 × 3) from five shops of three different markets of District Peshawar, Khyber Pakhtunkhwa, Pakistan. Before use, the subject samples were cleaned from all dust, powdered, and stored for further analysis.

### 2.2. Chemicals and instrumentation

Chemicals for elemental content; nitric acid ($HNO_3$), hydrogen peroxide ($H_2O_2$), ultra-pure deionized water, multi-element standards (1000 mg/L and 10 mg/L), and standard reference material were purchased from Fine-Chem (Korea), Millipore (USA), Perkin Elmer (USA) and National Institute of Standards and Technology, NIST (USA). Silver nitrate ($AgNO_3$), $CuSO_4{\cdot}5H_2O$, and $NiCl_2$ for PLNPs synthesis, DU-145 (prostate cancer cell line), L-929 (normal fibroblasts), 2,2-diphenyl-1-picrylhydrazyl (DPPH), 2′-azino-bis-3-ethyl benzthiazoline-6-sulphonic acid (ABTS), gallic acid, sodium borohydride ($NaBH_4$), and dyes were purchased from Sigma-Aldrich (Steinheim, Germany) and Merck (Darmstadt, Germany). Food colors were purchased from supermall Peshawar. Microbial strains; *Staphylococcus aureus* (ATCC 29213), *Bacillus subtilis* (ATCC 19659), *Pseudomonas aeruginosa* (ATCC 17588), *Escherichia coli* (ATCC 25922), *Candida albicans* (ATCC90029), *Candida krusei* (ATCC6258), *Aspergillus flavus* (ATCC9807), and *Trichophyton mentagrophytes* (ATCC40004), nutrient agar (Muller Hinton Broth), *p*-iodonitrotetrazolium chloride (INT), vancomycin, strepto-

mycin, fluconazole, and amphotericin were purchased from Oxoid (England) and Sigma-Aldrich (USA). Samples for elemental analysis were prepared using microwave digestion system (Topwave 3000, Austria) and analyzed by ICP-OES (Optima 8000) and ICP-MS (quadrupole Elan DRC II). FT-IR spectral analysis was performed on Bruker FT-IR spectrometer. The formation of PLNPs was detected by Shimadzu UV–Vis spectrophotometer (UV-1800). Shape and size of PLNPs were examined by scanning electron microscope (JSM-5910) and atomic force microscope (Bruker Corporation, Billerica, MA, USA). Nomenclature of the materials used in the study is given in Table 1.

### 2.3. *P. longum* samples preparation for elemental content

For elemental analysis, *P. longum* catkin samples were prepared following the published procedures of Hwang et al. (2016) and (2017). The microwave-assisted digested samples were then analyzed for elemental content determination by ICP-OES and ICP-MS techniques. The techniques were validated through quality parameters, SRM analysis, and participation in accredited laboratory proficiency test (FAPAS).

### 2.4. Preparation of *P. longum* aqueous extract (PLAE)

Aqueous extract was prepared by macerating 25,0 g powdered sample in 250 mL deionized water (1 g/10 mL), heated, and stirred at 40 °C and 500 rpm for 2 h. The extract was filtered, and stored in refrigerator for further analysis.

### 2.5. Synthesis of PLNPs

PLAgNPs were synthesized using PLAE and $AgNO_3$ solution (1 mM) mixed in different ratios (1:1–1:6) (Fig. S1, supplementary material). PLCuONPs and PLNiNPs were synthesized by mixing PLAE, $CuSO_4{\cdot}5H_2O$ (1 mM), and $NiCl_2$ (1 mM) solutions in 1:1–1:10 ratios under the conditions of incubation, stirring, heating and stirring, and by exposing the mixture to sunlight. The formation of PLNPs was confirmed by colorimetric assessment, and UV absorption peaks at specific wavelengths ranging from 400 to 435 nm (AgNPs), and 260 to 380 nm (CuONPs, NiNPs).

**Table 1** Nomenclature of the materials used in the current study.

| Abbreviations | Full Name |
|---|---|
| AgNPs | Silver nanoparticles |
| BR | Bright red |
| CR | Congo red |
| CuONPs | Copper oxide nanoparticles |
| DG | Deep green |
| MB | Methylene blue |
| MNPs | Metal nanoparticles |
| NiNPs | Nickel nanoparticles |
| NPs | Nanoparticles |
| PLAE | *Piper longum* aqueous extract |
| PLAgNPs | *Piper longum* silver nanoparticles |
| PLCuONPs | *Piper longum* copper oxide nanoparticles |
| PLNiNPs | *Piper longum* nickel nanoparticles |
| PLNPs | *Piper longum* nanoparticles |
| ZY | Zarda yellow |

### 2.6. Effect of pH, concentration of salt, and time on the synthesis of PLNPs

To determine pH effect on PLNPs, the solutions were made acidic and basic (pH 1 to 12) (Fig. S2, supplementary material). The nanoparticles were synthesized by mixing different ratios of PLAE and salt solutions, which were then analyzed at different time intervals of 0 to 240 min. After that, NPs were collected by centrifugation at 4000 rpm × g. The stability of NPs was examined at the times ranging from one to 18 days. The final product was dried in vacuum oven for 3 h, and stored in airtight vail for further analysis.

### 2.7. Characterization of PLNPs

The synthesized PLNPs were characterized by UV–Vis, FT-IR, SEM and AFM techniques for the determination of the functional groups and the size of the subject PLNPs. For SEM analysis, the samples were dispersed in distilled water, and sonicated for an hour. SEM micrographs of the synthesized NPs were taken using the JSM-5910 SEM machine. A thin film of each sample was prepared on SEM grid by just dropping a small amount of sample on the grid. The excess solution was removed from the sample using a blotting paper. The samples on the grid were allowed to dry under a mercury lamp for 5 min. Finally, the samples were gold-coated through sputter coater. AFM is an advanced technique with a reach that is swiftly increasing into the nanomaterials and biomedical fields. A sample concept and advanced machinery has made possible the application of AFM imaging to a wide range of materials (Ţălu et al. 2014). AFM analysis of surface topography were carried out in ambient conditions using a multimode AFM with Nanoscope IIIa controller (Bruker Corporation, Billerica, MA, USA) and a vertical engagement (JV) 125 μm scanner. Contact mode was used throughout the experiments, using silicon–nitride tips (NP-20, Bruker, nominal frequency 56 kHz, nominal spring constant of 0.32 N/m) and a scan resolution of 512 samples per line. The processing and analysis of images was done by NanoScope™ software (version V614r1; Digital Instruments, Tonawanda, NY, USA).

### 2.8. Anticancer, antioxidant, antibacterial, and antifungal activities of PLAE and PLNPs

Anticancer activity of the synthesized PLNPs was analyzed using LDH assay (Jamila et al. 2014a). The solutions (100 μg/mL) of PLNPs were prepared in DMSO. To determine the anticancer potential of the PLNPs against DU-145 and L-929 cell lines, a cytotoxicity detection kit measuring the amount of lactate dehydrogenase (LDH) released by damaged cells into the cell culture supernatant post-treatment was used. Antioxidant activity in the concentration ranges of 50–1000 μg/mL was evaluated by DPPH and ABTS radical scavenging assays (Jamila et al. 2014b). The results of radical scavenging ability of PLNPs were expressed as $IC_{50}$ calculated in Graphpad Prism 7. Antimicrobial activities were evaluated using Muller-Hinton agar (MHA) and broth (MHB) microdilution methods (Eloff, 1998; Zagoda & Porter, 2001). In disc

difusion assay, an inoculum (100 µL) was streaked on the Mueller–Hinton agar surface using a sterile cotton swab. Then, sterile paper disc impregnated with 20 µL PLNPs (2000 µg/mL), and the standard drugs (streptomycin, vancomycin, fluconazole, amphotericin) were kept on the inoculated agar. These were then incubated (37 °C) for 24 h. The diameters of inhibition zone were then measured in millimeters (mm). Besides, broth microdilution assay or minimal inhibitory concentration (MIC) in the concnetrarion range of 1000–31.25 µg/mL using sterile flat-bottom 96-well plate was performed. The bacterial strains were *Bacillus subtilis*, *Staphylococcus aureus*, *Escherichia coli* and *Pseudomonas aeruginosa* whereas yeasts included *Candida albicans*, *Candida krusei*, *Aspergillus flavus,* and *Trichophyton mentagrophytes*.

### 2.9. Redox catalytic potential of PLNPs

An equal volume of $NaBH_4$ solution (100 mM) and dyes were mixed. The solutions were then made up to 10 mL using deionized water, and stirred for 5 min. Then, 1 mL of PLNPs was added to the each reaction mixture, and stirred for 5 more min. Decolorization of reaction solution and disappearance of absorption maxima indicated the degradation of dyes. The reaction unsupported by the catalyst was taken as a reference.

### 2.10. Statiscal analysis

The obtained results of elemental content and antimicrobial activities are reported as means ± standard deviations ($n = 3$). The mean significant differences (represented by superscript letters) between the obtained values were analyzed using ANOVA along with Tukey's HSD test in SPSS, version 20.0 (SPSS Inc., Chicago, USA). The $IC_{50}$ values were calculated with the help of GraphPad Prism 7 (GraphPad Software Inc., La Jolla, USA). Data are expressed with a significance level of $p < 0.05$.

## 3. Results and discussion

### 3.1. Analytical performance of ICP-OES and ICP-MS for elemental content

The obtained results of linearity, precision, accuracy, and FAPAS (Tables S1-S3, supplementary material) represented the suitability of the applied procedures and thus, confirmed that the applied methods fulfill the required criteria of Association of Official Analytical Chemists (2012) (Poitevin, 2012).

### 3.2. Elemental concentrations in P. longum catkin

In most cases, herbs are indiscriminately collected from non-cultivated and non-ecofriendly areas, and brought to the market without any quality control. This may lead to the exposure of consumers to contaminated (pesticides, toxic metals, mycotoxins, adulterated with drugs) products. However, ideally, herbs and their products should be strictly quality checked in terms of contamination from toxic metals. Consumers have increased interest to choose the diet having high nutrient levels, preferably from natural sources. Considering the scientific and consumers demand, this study determined the content of

**Table 2** Mean and ranges of the concentrations (µg/g) of the analyzed elements in *P. longum* catkin.

| Macro elements | | | | | | | | |
|---|---|---|---|---|---|---|---|---|
| Al | Ca | Fe | K | Mg | Na | P | S | |
| 1.08 ± 0.063 | 147.8 ± 7.63 | 1.24 ± 0.072 | 507.2 ± 6.55 | 41.0 ± 1.87 | 11.0 ± 2.36 | 53.6 ± 0.589 | 7.64 ± 0.198 | |
| 0.693–2.75 | 101.9–165.7 | 0.776–2.54 | 433.6–574.9 | 29.7–68.2 | 5.73–19.5 | 38.5–61.6 | 5.47–9.53 | |
| *Micro elements* | | | | | | | | |
| $Ni^{60}$ | $Cu^{63}$ | $Zn^{64}$ | $Sr^{87}$ | $Rb^{85}$ | | | | |
| 0.051 ± 0.002 | 0.156 ± 0.002 | 0.398 ± 0.010 | 6.85 ± 0.046 | 7.58 ± 0.057 | | | | |
| 0.017–0.116 | 0.072–0.201 | 0.211–0.507 | 4.29–9.06 | 3.99–9.51 | | | | |
| *Trace essential elements* | | | | | | | | |
| $V^{51}$ | $Cr^{52}$ | $Cr^{53}$ | $Co^{59}$ | $Se^{82}$ | | | | |
| 0.003 ± 0.0008 | 0.015 ± 0.0005 | 0.011 ± 0.0002 | 0.001 ± 0.00001 | 0.0002 ± 0.00007 | | | | |
| 0.0009–0.004 | 0.007–0.020 | 0.005–0.064 | 0.0004–0.002 | 0.00014–0.0003 | | | | |
| *Trace non-toxic elements* | | | | | | | | |
| $Li^7$ | $Be^9$ | $Ga^{6379}$ | | | | | | |
| 0.002 ± 0.0001 | ND | 0.003 ± 0.0002 | | | | | | |
| 0.0007–0.003 | ND | 0.0007–0.004 | | | | | | |
| *Trace toxic elements* | | | | | | | | |
| $As^{75}$ | $Cd^{111}$ | $In^{115}$ | $Cs^{133}$ | $Ba^{138}$ | $Tl^{205}$ | $Pb^{206}$ | $Pb^{208}$ | $U^{238}$ |
| 0.001 ± 0.0002 | 0.0001 ± 0.00002 | 0.0003 ± 0.00001 | 0.003 ± 0.0001 | 0.178 ± 0.013 | 0.00002 ± 0.000002 | 0.008 ± 0.0007 | 0.007 ± 0.0006 | 0.00009 ± 0.000004 |
| 0.0004–0.002 | 0.00005–0.0002 | 0.00007–0.0004 | 0.002–0.0037 | 0.096–0.215 | 0.00000–0.00004 | 0.005–0.009 | 0.005–0.016 | 0.00000–0.00017 |

macro and micronutrients, and toxic elements in *P. longum* catkin consumed in Pakistan. Among the content of macro-elements (Table 2), K was present at high level (507.2 µg/g), followed by Ca (147.8 µg/g). Plants are considered as potential source of essential micro-elements such as Cu, Cr, Ni, Mn and Zn, having significant role in several metabolic and biological processes. However, their presence above the permissible limits could cause toxicity to living system. Among the analyzed microelements (Table 2), $Rb^{85}$ (7.58 µg/g) and $Sr^{87}$ (6.85 µg/g) had high content. Among the essential elements; Co, Cr, Mn, Se, and V, which are important cofactors during metabolic processes, the content of $Cr^{52}$ was high (0.015 µg/g) followed by $V^{51}$. Relating the content of trace non-toxic elements; $Li^{7}$, $Be^{9}$, $Ga^{69}$, $Cs^{133}$, and $Ba^{138}$ (Table 2), $Ba^{138}$ was high followed by $Ga^{69}$ and $Cs^{133}$.

In common, herbal preparations and products are directly sold in the market without passing through safety evaluation, which may cause any adverse effects due to the presence of toxic elements. Therefore, it is necessary to evaluate the toxic/heavy metals in herbs and their products. *P. longum* catkin contained Pb and As (Table 2) below the permissible values. In the curret study, elemental content variations were found when the results compared with the literature (Ernst, 2002; Bhat et al. 2010; Meena et al. 2010).

### *3.3. Synthesis and effect of pH, salt concentration and time on PLNPs*

Present investigation describes the green synthesis of AgNPs, CuONPs, and NiNPs using PLAE, acting as reducing as well as stabilizing agent during synthesis. Metal ions ($Ag^{+}$, $Cu^{+2}$, $Ni^{+2}$) oxidize the hydroxyl groups of phytoconstituents to carbonyl groups and, thus, reducing metals to elemental form ($Ag^{0}$, $Cu^{0}$, $Ni^{0}$). PLNPs of Ag, CuO and Ni were synthe-

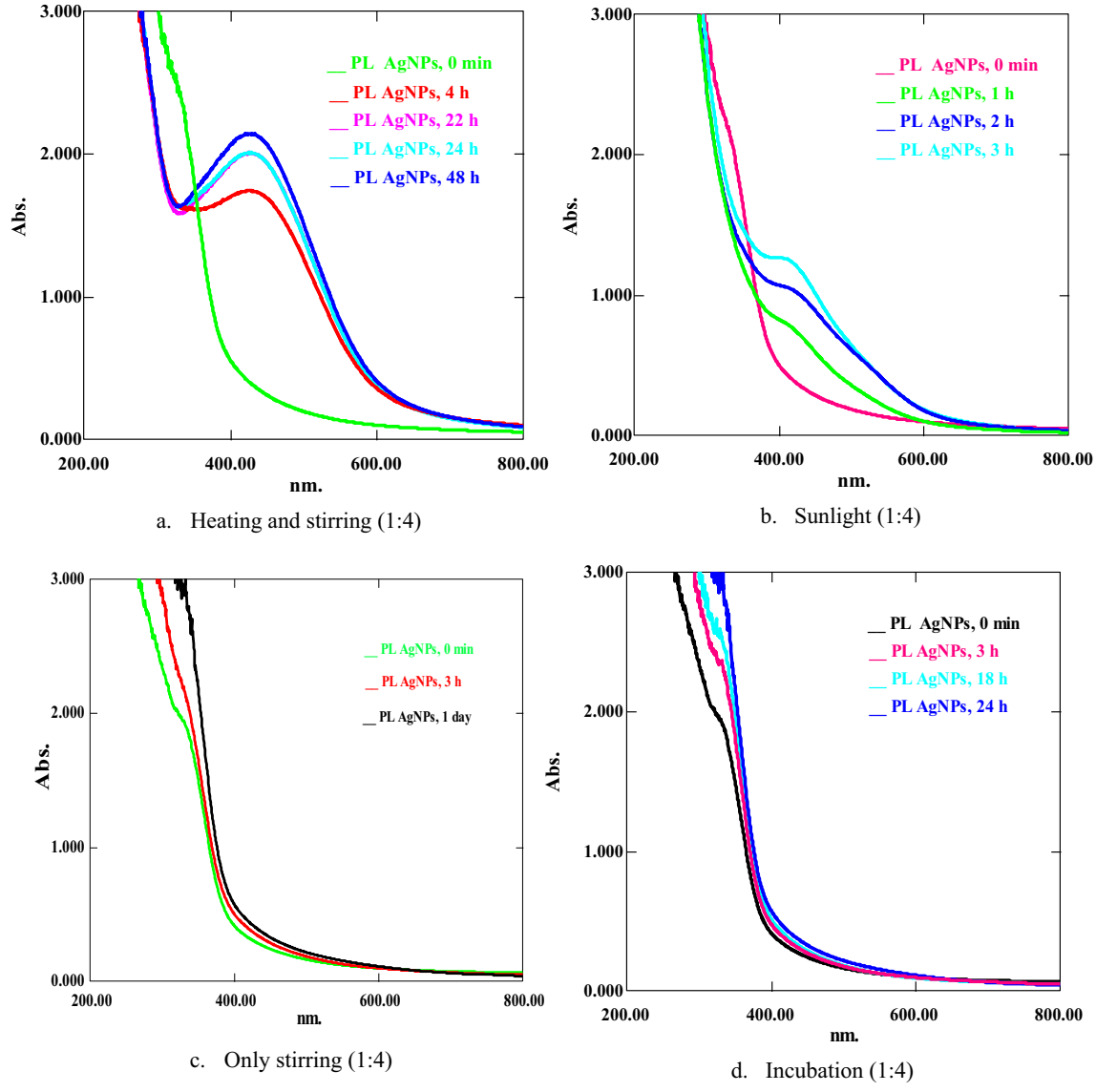


a. Heating and stirring (1:4)

b. Sunlight (1:4)

c. Only stirring (1:4)

d. Incubation (1:4)

**Fig. 1** UV spectra of PLAgNPs (1:4) under (a) heating and stirring, (b) sunlight, (c) stirring, and (d) incubation at room temperature.

sized in different ratios ranging from 1:1 to 1:10 (PLAE:1 mM salt solution) under stirring, heating and stirring, incubation, and sunlight. Colorimetric changes and appearance of absorption peaks at 420–435 nm for PLAgNPs, and 260–380 nm for PLCuONPs and PLNiNPs indicated the formation of NPs (Reddy et al. 2014; Rajan et al. 2015; Jayapriya et al. 2019; Tripathi et al. 2019; Yadav et al. 2019). In case of PLAgNPs, no NPs were formed with 1:1 to 1:3 ratios (Fig. S3, supplementary material). However, ratios 1:4 to 1:6 uniformly stirred at 60 °C, resulted in AgNPs formation. This reaction mixture exhibited an absorption peak at 420 nm, corresponding to the typical surface Plasmon resonance (SPR) of conducting electrons from the surface of AgNPs (Kumar et al. 2016; Khan et al. 2018). Hence, further NPs were synthesized with the subject ratios under different conditions. For example, in 1:4 siratio, AgNPs were formed in a high content under heating and stirring (Fig. 1), while by applying sunlight, a very small amount of AgNPs were formed. However, at other conditions, no AgNPs were formed. Similarly, 1:5 ratio resulted in rapid AgNPs formation under stirring, incubation and exposure to sunlight, whereas in this ratio, under heating and stirring, no AgNPs were formed (Fig. 2). In 1:6 ratio, AgNPs were formed under stirring as well as by incubating the mixture (Fig. 3). Previously *P. longum* leaf extract AgNPs were synthesized only under incubation in dark in 1:9 ratio (Jacob et al. 2012). However, in the present study, PLAgNPs are synthesized in a wide range of ratios under different conditions, which indicated that depending upon the concentration of salt solution, AgNPs can be synthesized using the conditions of stirring, heating, incubation or sunlight.

In the synthesis of PLCuONPs, ratios 1:1–1:4 did not give any NPs formation (Fig. S4, supplementary material), whereas proceeding with 1:5–1:9 mixtures, a formation of CuONPs observed and absorption peaks at 270 nm appeared, which indicated the existence of PLCuONPs (Fig. S5, supplementary material). Furthermore, with 1:10 ratio, a rapid formation of PLCuONPs occurred with prominent absorption peak at 270 nm representing significant NPs content. Thus, further nanoparticles in this ratio were synthesized under incubation, stirring, heating and stirring, and exposing to sunlight in which PLCuONPs were prominently formed at heating (60 °C) and stirring (500 rpm) for 1 to 2 h (Fig. 4). UV spectra of

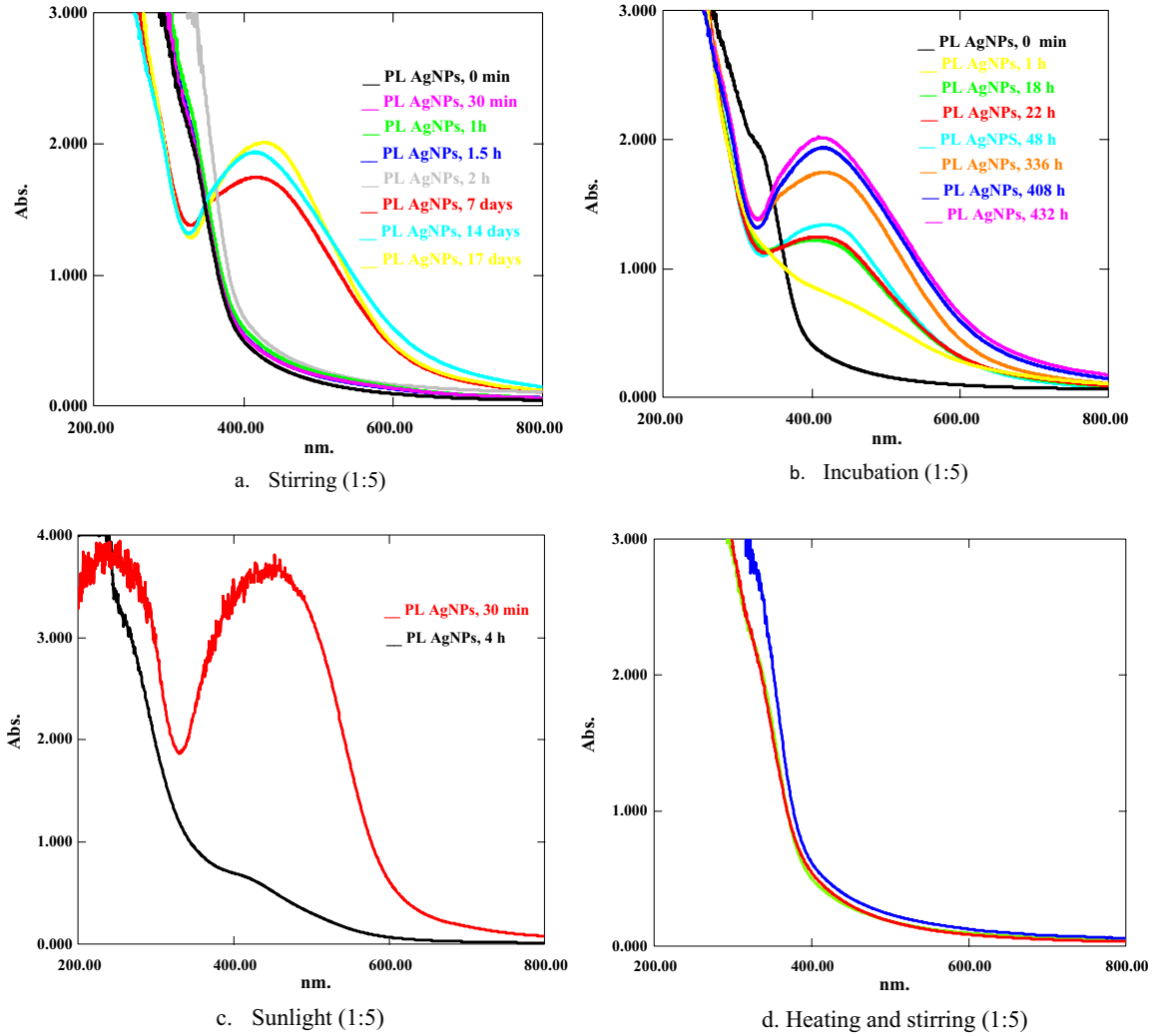


a. Stirring (1:5)

b. Incubation (1:5)

c. Sunlight (1:5)

d. Heating and stirring (1:5)

**Fig. 2** UV spectra of PLAgNPs (1:5) under (a) heating and stirring, (b) sunlight, (c) stirring, and (d) incubation at room temperature.

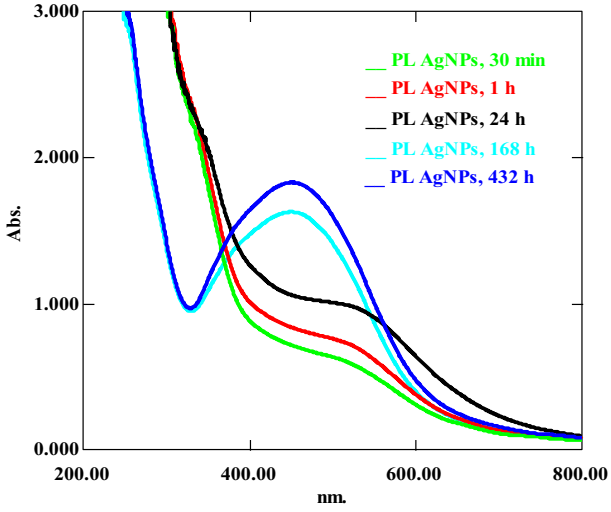


a. Stirring (1:6)

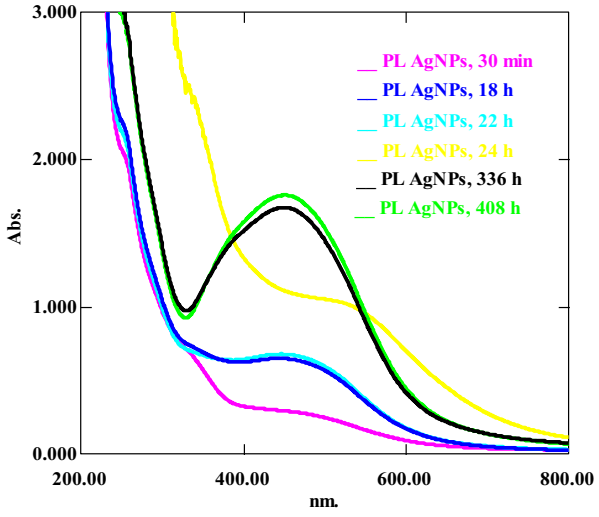


b. Incubation (1:6)

**Fig. 3** UV spectra of PLAgNPs (1:6) under (a) stirring, and (b) incubation at room temperature.

PLCuONPs contain one strong and a week peak located at 270 and 335 nm, respectively confirming the formation of PLCuONPs (Katwal et al. 2015).

Regarding PLNiNPs, ratios from 1:1 to 1:3 did not result in NPs formation (Fig. S6, supplementary material), whereas using 1:4 to 1:9 ratio, small peaks at 260 nm and 335 nm appeared, which indicated NiNPs formation in lesser amount (Fig. S7, supplementary material). However, using 1:10 ratio, prominent absorption peaks at 260 nm and 335 nm were observed (Fig. 5). Hence, in the current study, it was found that under heating and stirring, *P. longum* catkin aqueous extract could predominantly yield the most stable and well dispersed NPs in the highest content as compared to the methods previously published on *P. longum* leaf and catkin aqueous extract AgNPs (Jacob et al. 2012; Reddy et al., 2014; Jayapriya et al. 2019; Yadav et al. 2019).

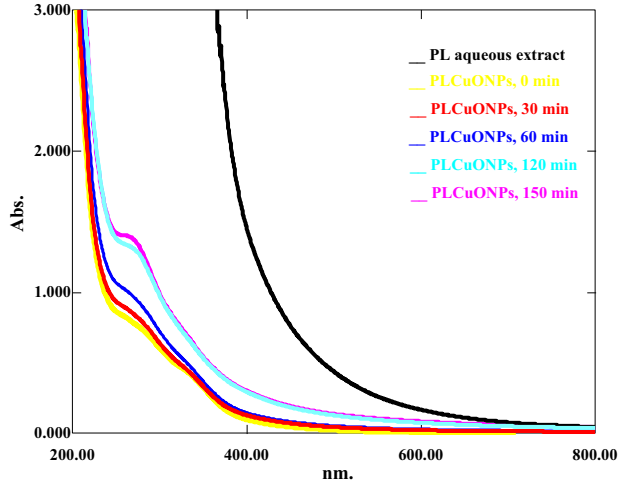


a. Heating and stirring (1:10)

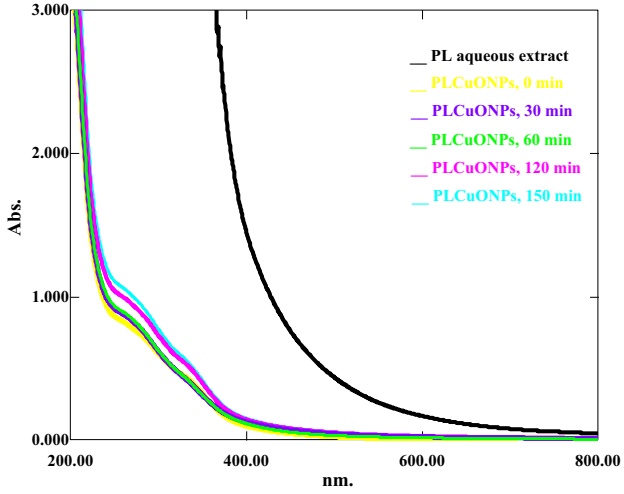


b. Stirring (1:10)

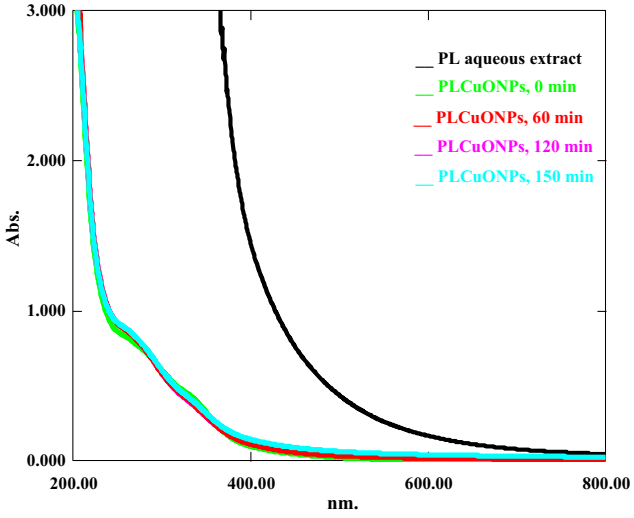


c. Sunlight (1:10)

**Fig. 4** UV spectra of PLCuONPs (1:10) under (a) [heating (60 °C) and stirring (500 rpm)], (b) stirring, and (c) sunlight.

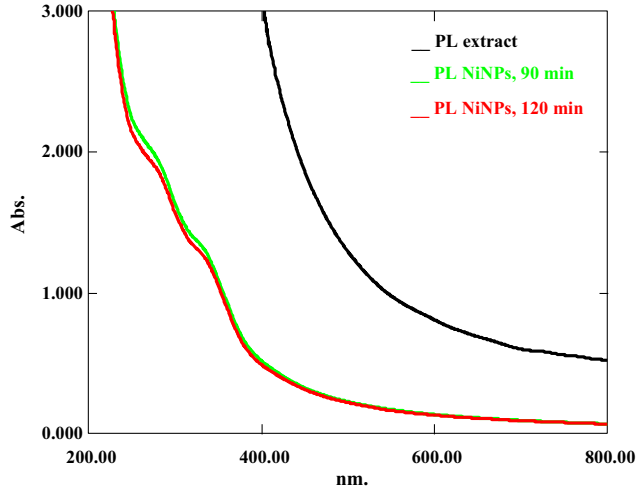


a. Heating and stirring (1:10)

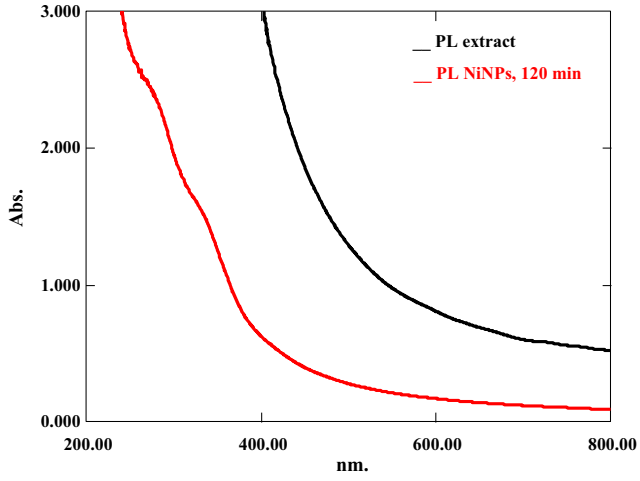


b. Stirring (1:10)

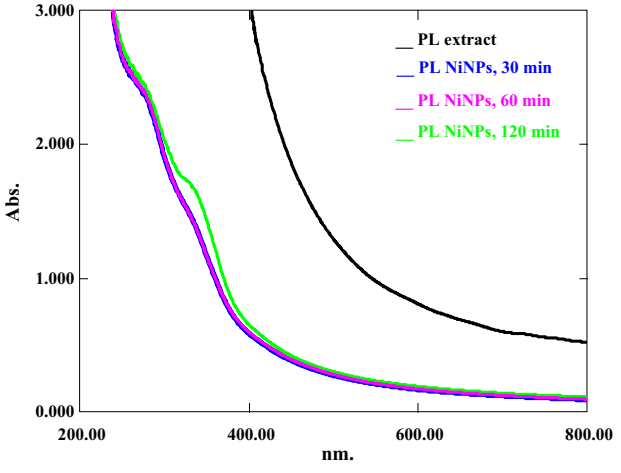


c. Sunlight (1:10)

**Fig. 5** UV spectra of PLNiNPs (1:10) under (a) [heating (60 °C) and stirring (500 rpm)], (b) stirring, and (c) sunlight.

A pH of the reaction mixture is another parameter, which plays a vital role in the manipulation of surface morphology, shape, size, texture, and aggregation of NPs (Yadav et al. 2019). A change in absorption peak intensity and wavelength was recorded on varying pH of the reaction mixture (1.5 to 13) as shown in Fig. S8 (supplementary material). Regarding the AgNPs synthesized with 1:4 ratio, a red shift in absorption maximum was observed from 420 nm to 440 nm, at highly acidic pH (1.5), whereas sharp intense absorption peaks were obtained under slightly neutral to highly basic conditions (pH 6 to 13). At pH 3, a flat spectrum of SPR and no change in the color of the reaction mixture was observed. Proceeding to 1:5 ratio, the most intense and sharp peak was observed with pH 10, whereas for 1:6, no prominent effect on NPs synthesis was observed. Our observations suggested that for 1:4 and 1:5 biosynthesized AgNPs, pH 6 and 10 were optimum, whereas there is no significant effect of pH on 1:6 biosynthesized AgNPs. For PLCuONPs and PLNiNPs, pH 7 and 8 were found optimum.

### *3.4. Characterization of PLNPs*

The functional groups involved in the reduction of metal ions to elemental form were determined by FT-IR studies in which the spectra of PLAE and PLNPs were found similar but with differences of reduced intensities in specified absorptions (Fig. S9(a-d)). PLAE spectrum exhibited prominent peaks at 3500–3200 $cm^{-1}$, 2900–2800 $cm^{-1}$, 1750–1600 $cm^{-1}$. These peaks are attributed to the stretching of N–H, O–H, C–H, and C═O of secondary metabolites present in *P. longum* catkin extract. The reduced absorption and shape changes at 3500–3200 $cm^{-1}$ and 1750–1600 $cm^{-1}$ indicate the involvement and interaction of these absorptions in the formation of PLNPs. The size and shape morphology of the synthesized PLNPs were determined by SEM and AFM analysis. From SEM images (Fig. 6a-c), it is observed that the surface morphology of PLAgNPs have spherical shapes. Fig. 6d-i shows two-dimensional AFM images of the synthesized PLNPs. From the micrographs, it is evident that surface morphologies of the PLNPs were rough. The shapes of particles did not show any significant difference, most of the particles possessed spherical shapes. Furthermore, the NPs were well dispersed without aggregation. The average diameter of the PLNPs was in the range of 67–83 nm. PLAgNPs possessed the smallest size (67 nm), while PLCuONPs and PLNiNPs possessed comparative large sizes 83 and 78 nm, respectively.

### *3.5. Anticancer, antioxidant, antibacterial, and antifungal activities of PLAE and PLNPs*

The PLNPs prominently formed in high content such as, PLAgNPs in 1:4 ratio, and PLCuONPs and PLNiNPs in 1:10 ratio under heating and stirring were subjected to anticancer, antioxidant, antimicrobial, and redox catalytic assessment. In anticancer activity, the ability of PLNPs to induce DU-145 human prostate cancer and L-929 (normal fibroblasts) cells death was tested for the first time. From the results, it was

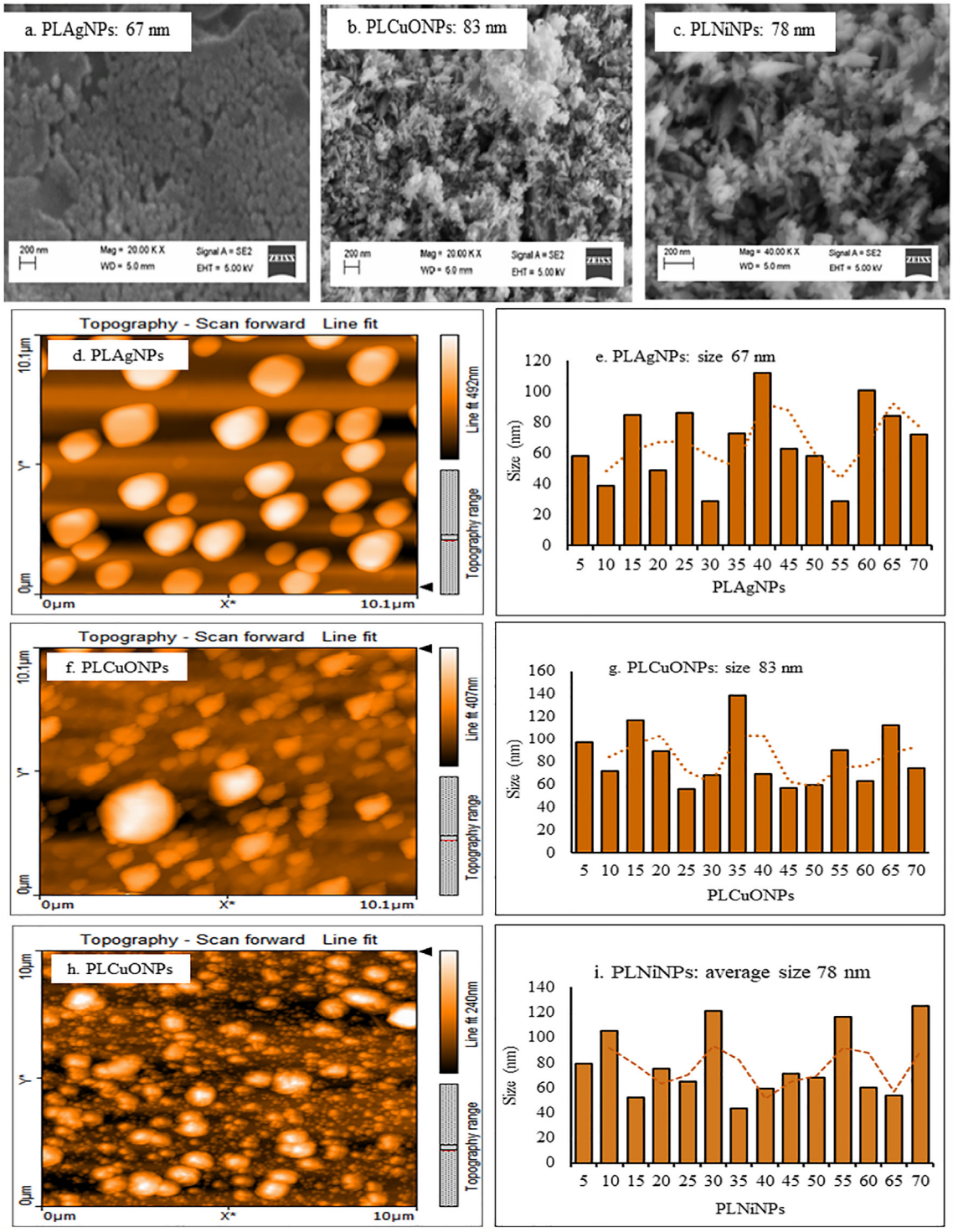


**Fig. 6** SEM (a-c), and AFM images and particle size distribution graphs (d-i) of the synthesized PLAgNPs (1:4), PLCuONPs (1:10), and PLNiNPs (1:10) under heating and stirring.

found that all the synthesized PLNPs at 100 µg/mL were toxic towards DU-145 cells in which PLAgNPs and PLNiNPs induced 100% cell death after 72 h of treatment of the DU-145 cells, followed by PLCuONPs with 92.67% (Fig. 7). At the same concentration and incubation period, PLAE showed low cytotoxic effect with 55.82% cell death, which concluded that compared to the PLAE, its NPs have more cytotoxic potential. It was further observed that cytotoxicity against nor-

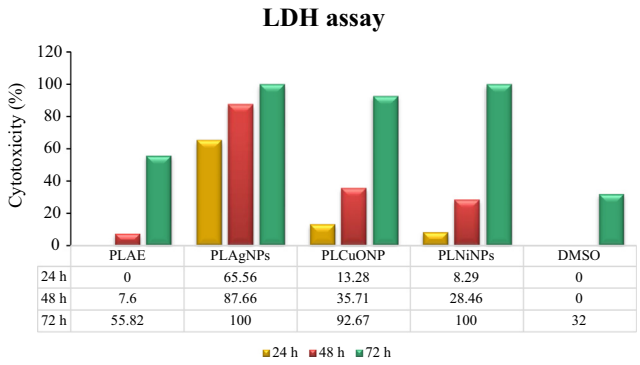


**Fig. 7** Percent (%) cytotoxicity (LDH assay) of PLAE, PLAgNPs (1:4), PLCuONPs (1:10), and PLNiNPs (1:10) under heating and stirring, tested on DU-145 cells.

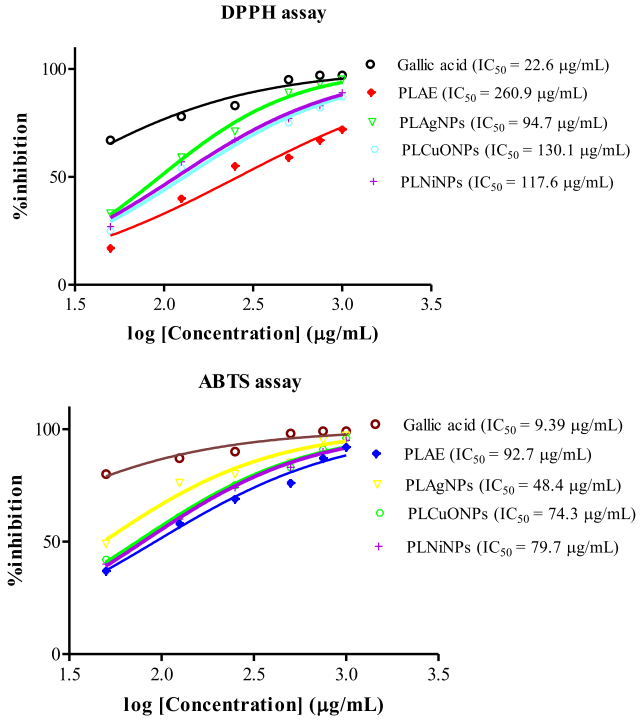


**Fig. 8** . Antioxidant activity (DPPH and ABTS assays) of PLAE and synthesized PLNPs.

mal cells (L-929) was lower (1–2%) as compared to DU-145, which might indicates a selective action of PLNPs on cancer cells. In antioxidant activity (Fig. 8), among the analyzed samples, PLAgNPs are comparatively potent inhibitors of the DPPH showing $IC_{50}$ values of 94.7 µg/mL, as compared to other NPs. The $IC_{50}$ values of PLCuONPs and PLNiNPs were 130.1 and 117.6 µg/mL, respectively. In ABTS assay, PLAgNPs exhibited the highest ability to scavenge ABTS radical ($IC_{50}$ of 48.4 µg/mL), followed by PLCuONPs, PLNiNPs, and PLAE, respectively. From the nonlinear graph, it is observed that the inhibition of DPPH and ABTS radicals is dose-dependent, which increases with increasing concentration of PLNPs. In antibacterial activity, (Table 3), PLAE as compared to PLNPs has shown weak inhibition against the tested bacterial strains with inhibition zone of 7.0 to 13.0 mm and minimum inhibitory concentration (MIC) values of 500 to 1000 µg/mL. Among the PLNPs, PLAgNPs were the most active NPs against both the Gram-positive and negative bacterial strains, having inhibition zones of 16–24 mm and MIC values of 31.25 to 250 µg/mL higher than the standard (vancomycin). Furthermore, PLCuONPs inhibited *S. aureus* with higher inhibition zone (19.0 mm) as compared to vancomycin. This significant antibacterial action of the synthesized NPs could be due to the reactive oxygen species (ROS) produced and involve in the bactericidal activity of nanoparticles (Khan et al. 2018). Similar to antibacterial activity, in antifungal activity (Table 3), PLAgNPs shows pronounced inhibitory effects against more than one fungal species giving inhibitory zones of 15–21 mm and MIC values of 31.25 to 250 µg/mL.

### *3.6. Redox catalytic potential of PLNPs*

Dyes can be degraded by reducing agents such as $NaBH_4$ to non-toxic species, but kinetically the rate is very slow. Metal nanoparticles having high surface area can enhance the reducing efficiency (Vidhu & Philip, 2014). In this research work, several dyes and food colors were reduced with $NaBH_4$ in the presence of PLNPs. From the results (Fig. S10, supplementary material), it can be seen that $NaBH_4$ added dyes (MB, CR, DG, ZY, BR) without any PLNPs show a small change in the absorbance of dyes, which indicates slow reduction by $NaBH_4$. However, in the presence of PLNPs, the prominent absorption peaks of dyes disappeared. This might be due to the adsorption between PLNPs and dyes, enhancing the redox process between the active dyes and $NaBH_4$.

## 4. Conclusions

This study reports the elemental determination of *P. longum* catkin, synthesis, characterization, and biological activities assessment of its synthesized silver, copper oxide and nickel nanoparticles. The content of nutritional (macro, micro and essential trace) elements in the analyzed catkin are present at appreciable amounts, which could meet the nutritional requirements of consumers. The content of toxic elements were below the provisional tolerable intake and lethal limits. PLAgNPs were significantly synthesized in 1:4 ratio, whereas PLCuONPs and PLNiNPs in 1:10 ratio under heating and stirring. The optimum pH range for the subject NPs was 6–10. In addition, PLNPs showed relevant cytotoxicity against prostate cancer line; DU-145 cell line compared to normal human cells, which could be indicative of selective action of the subject NPs on cancer cells. Furthermore, the synthesized PLNPs have shown significant antioxidative and antimicrobial potential. In addition, PLNPs acted as active redox catalysts in dyes degradation. Hence, conclusively, *P. longum* catkin could be significant source of mineral nutrients and safe for human consumption. The synthesized PLNPs could be effective therapeutic agents in diseases involving free radicals, and beneficial in eco-friendly environmental remediation of organic pollutants.

**Table 3** Antibacterial and antifungal activities by disc diffusion (zone of inhibition, mm) and minimum inhibitory concentration (MIC, μg/mL) methods of *P. longum* catkin extract and synthesized nanoparticles.

| Antibacterial activity | | | | | | | | |
|---|---|---|---|---|---|---|---|---|
| Samples | Disk diffusion (zone of inhbition, mm) | | | | Minimum inhibitory concentration (μg/mL) | | | |
| | *S. aureus* | *B. subtilis* | *P. aeruginosa* | *E. coli* | *S. aureus* | *B. subtilis* | *P. aeruginosa* | *E. coli* |
| PLAE | $13.0^{a} \pm 0.15$ | $12.0^{a} \pm 0.24$ | $8.0^{a} \pm 0.39$ | $7.0^{a} \pm 0.10$ | $500^{c}$ | $500^{c}$ | $1000^{c}$ | $1000^{c}$ |
| PLAgNPs | $23.0^{e} \pm 0.31$ | $24.0^{c} \pm 0.57$ | $17.0^{e} \pm 0.62$ | $16.0^{d} \pm 0.29$ | $31.25^{a}$ | $31.25^{a}$ | $250^{a}$ | $250^{a}$ |
| PLCuONPs | $19.0^{d} \pm 0.28$ | $17.0^{b} \pm 0.33$ | $14.0^{c} \pm 0.36$ | $15.0^{c} \pm 0.52$ | $62.5^{b}$ | $62.5^{b}$ | $500^{b}$ | $500^{b}$ |
| PLNiNPs | $15.0^{b} \pm 0.51$ | $12.0^{a} \pm 0.15$ | $13.0^{bc} \pm 0.33$ | $15.0^{c} \pm 0.41$ | $62.5^{b}$ | $62.5^{b}$ | $500^{b}$ | $500^{b}$ |
| Vancomycin* | $18.0^{c} \pm 0.47$ | $26.0^{d} \pm 0.45$ | $12.0^{b} \pm 0.40$ | $13.0^{b} \pm 0.27$ | $31.25^{a}$ | $31.25^{a}$ | $500^{b}$ | $250^{a}$ |
| Streptomycin* | $18.0^{c} \pm 0.20$ | $26.0^{d} \pm 0.61$ | $16.0^{d} \pm 0.19$ | $18.0^{e} \pm 0.39$ | $31.25^{a}$ | $31.25^{a}$ | $500^{b}$ | $500^{c}$ |
| *Antifungal activity* | | | | | | | | |
| Samples | Disk diffusion (mm) | | | | Minimum inhibitory concentration method (μg/mL) | | | |
| | *C. albicans* | *C. krusei* | *A. flavus* | *T. mentagrophytes* | *C. albicans* | *C. krusei* | *A. flavus* | *T. mentagrophyte* |
| PLAE | $13.0^{a} \pm 0.29$ | $9.0^{a} \pm 0.16$ | $11.0^{a} \pm 0.33$ | $9.0^{a} \pm 0.18$ | $250^{c}$ | $1000^{d}$ | $500^{c}$ | $1000^{c}$ |
| PLAgNPs | $21.0^{d} \pm 0.10$ | $17.0^{d} \pm 0.23$ | $17.0^{d} \pm 0.42$ | $15.0^{c} \pm 0.55$ | $31.25^{a}$ | $250^{b}$ | $62.5^{a}$ | $250^{a}$ |
| PLCuONPs | $18.0^{b} \pm 0.62$ | $13.0^{c} \pm 0.32$ | $14.0^{c} \pm 0.37$ | $15.0^{c} \pm 0.28$ | $62.5^{b}$ | $500^{c}$ | $250^{b}$ | $250^{a}$ |
| PLNiNPs | $18.0^{b} \pm 0.24$ | $12.0^{b} \pm 0.28$ | $12.0^{b} \pm 0.16$ | $13.0^{b} \pm 0.49$ | $62.5^{b}$ | $500^{c}$ | $500^{c}$ | $500^{b}$ |
| Fluconazole* | $20.0^{c} \pm 0.19$ | $23.0^{f} \pm 0.31$ | $28.0^{f} \pm 0.17$ | $30.0^{e} \pm 0.16$ | $31.25^{a}$ | $31.25^{a}$ | $62.5^{a}$ | $250^{a}$ |
| Amphotericin* | $20.0^{c} \pm 0.22$ | $20.0^{e} \pm 0.31$ | $21.0^{e} \pm 0.36$ | $23.0^{d} \pm 0.71$ | $250^{c}$ | $250^{b}$ | $250^{b}$ | $250^{a}$ |

Superscript letters (a-f) within the columns represent significant differences ($p < 0.05$) in the antibacterial and antifungal activities by disc diffusion (zone of inhibition, mm) and minimum inhibitory concentration (MIC, μg/mL) values of the synthesized nanoparticles and the standard drugs.

* Represents standard drugs.

## Acknowledgement

This research study was supported by the research grant; 8967/KPK/NRPU/R&D/HEC/2017. The authors are thankful to the Higher Education Commission (HEC) for awarding this project.

## Declaration of Competing Interest

The authors declare no conflict of interest.

## Appendix A. Supplementary data

Supplementary data to this article can be found online at https://doi.org/10.1016/j.arabjc.2020.06.001.

## References

Ali, F., Khan, S.B., Kamal, T., Anwar, Y., Alamry, K.A., Asiri, A.M., 2017. Anti-bacterial chitosan/zinc phthalocyanine fibers supported metallic and bimetallic nanoparticles for the removal of organic pollutants. Carbohyd. Polym. 173, 676–689. https://doi.org/10.1016/j.carbpol.2017.05.074.

Anwar, A., Minhaz, A., Khan, N.A., Kalantari, K., Afifi, A.B.M., Shah, M.R., 2018. Synthesis of gold nanoparticles stabilized by a pyrazinium thioacetate ligand: A new colorimetric nanosensor for detection of heavy metal Pd (II). Sens. Actuat. B-Chem. 257, 875–881. https://doi.org/10.1016/j.snb.2017.11.040.

Bello, B.A., Khan, S.A., Khan, J.A., Syed, F.Q., Anwar, Y., Khan, S. B., 2017. Antiproliferation and antibacterial effect of biosynthesized AgNps from leaves extract of *Guiera senegalensis* and its catalytic reduction on some persistent organic pollutants. J. Photochem. Photobiol. B-Biol. 175, 99–108. https://doi.org/10.1016/j.jphotobiol.2017.07.031.

Bhat, R., Kiran, K., Arun, A.B., Karim, A.A., 2010. Determination of mineral composition and heavy metal content of some nutraceutically valued plant products. Food Anal. Methods. 3, 181–187. https://doi.org/10.1007/s12161-009-9107-y.

Dhand, C., Dwivedi, N., Loh, X.J., Ying, A.N.J., Verma, N.K., Beuerman, R.W., Lakshminarayanan, R., Ramakrishna, S., 2015. Methods and strategies for the synthesis of diverse nanoparticles and their applications: a comprehensive overview. RSC Adv. 5, 105003–105037. https://doi.org/10.1039/C5RA19388E.

Eleftheriadou, M., Pyrgiotakis, G., Demokritou, N., 2017. Nanotechnology to the rescue: using nano-enabled approaches in microbiological food safety and quality. Curr. Opin. Biotechnol. 44, 87–93. https://doi.org/10.1016/j.copbio.2016.11.012.

Eloff, J.N., 1998. Which extractant should be used for the screening and isolation of antimicrobial components from plants?. J. Ethnopharmacol. 60, 1–8. https://doi.org/10.1016/S0378-8741(97)00123-2.

Ernst, E., 2002. Heavy metals in traditional Indian remedies. Eur. J. Clin. Pharmacol. 57, 891–896. https://doi.org/10.1007/s00228-001-0400-y.

Hwang, I.M., Choi, J.Y., Nho, E.Y., Dang, Y.M., Jamila, N., Khan, N., Kim, K.S., 2017. Determination of essential and toxic elements in vegetables from South Korea. Anal. Lett. 50, 663–681. https://doi.org/10.1080/00032719.2016.1194426.

Hwang, I.M., Yang, J.S., Kim, S.H., Jamila, N., Khan, N., Kim, K.S., Seo, H.Y., 2016. Elemental analysis of sea, rock, and bamboo salts by inductively coupled plasma-optical emission and mass spectrometry. Anal. Lett. 49, 2807–2821. https://doi.org/10.1080/00032719.2016.1158831.

Jacob, S.J.P., Finub, J.S., Narayanan, A., 2012. Synthesis of silver nanoparticles using *Piper longum* leaf extracts and its cytotoxic activity against Hep-2 cell line. Colloid Surf. B. 91, 212–214. https://doi.org/10.1016/j.colsurfb.2011.11.001.

Jamila, N., Khairuddean, M., Yaacob, S.S., Kamal, N.N.S.N.M., Osman, H., Khan, S.N., Khan, N., 2014a. Cytotoxic benzophenone and triterpene from *Garcinia hombroniana*. Bioorg. Chem. 54, 60–67. https://doi.org/10.1016/j.bioorg.2014.04.003.

Jamila, N., Khairuddean, M., Khan, S.N., Khan, N., 2014b. Complete NMR assignments of bioactive rotameric (3→8) biflavonoids from the bark of *Garcinia hombroniana*. Magn. Reson. Chem. 52, 345–352. https://doi.org/10.1002/mrc.4071.

Jayapriya, M., Dhanasekaran, D., Arulmozhi, M., Nandhakumar, E., Senthilkumar, N., Sureshkumar, K., 2019. Green synthesis of silver nanoparticles using *Piper longum* catkin extract irradiated by sunlight: antibacterial and catalytic activity. Res. Chem. Intermediat. 45, 3617–3631. https://doi.org/10.1007/s11164-019-03812-5.

Katwal, R., Kaur, H., Sharma, G., Naushad, M., Pathania, D., 2015. Electrochemical synthesized copper oxide nanoparticles for enhanced photocatalytic and antimicrobial activity. J. Ind. Eng. Chem. 31, 173–184. https://doi.org/10.1016/j.jiec.2015.06.021.

Khan, A., Khan, S.B., Kamal, T., Asiri, A.M., Akhtar, K., 2016. Recent development of chitosan nanocomposites for environmental applications. Recent Pat. Nanotech. 10, 181–188. https://doi.org/10.2174/1872210510666160429145339.

Khan, S.A., Bello, B.A., Khan, J.A., Anwar, Y., Mirza, M.B., Qadri, F., Farooq, A., Adam, I.K., Asiri, A.M., Khan, S.B., 2018. *Albizia chevalier* based Ag nanoparticles: Anti-proliferation, bactericidal and pollutants degradation performance. J. Photochem. Photobiol. B-Biol. 182, 62–70. https://doi.org/10.1016/j.jphotobiol.2018.03.020.

Khan, S.A., Ismail, M., Anwar, Y., Farooq, A., Al-Johny, B.O., Akhtar, K., Shah, Z.A., Nadeem, M., Raza, M.A., Khan, S.B., 2019. A highly efficient and multifunctional biomass supporting Ag, Ni, and Cu nanoparticles through wetness impregnation for environmental remediation. Green Process. Synth. 8, 309–319. https://doi.org/10.1515/gps-2018-0101.

Kumar, A., Panghal, S., Mallapur, S.S., Kumar, M., Ram, V., Singh, B.K., 2009. Anti-inflammatory activity of *Piper longum* fruit oil. Indian J. Pharm. Sci. 71, 454–456. https://doi.org/10.4103/0250-474X.57300.

Kumar, V., Singh, D.K., Mohan, S., Hasan, S.H., 2016. Photo-induced biosynthesis of silver nanoparticles using aqueous extract of *Erigeron bonariensis* and its catalytic activity against Acridine Orange. J. Photochem. Photobiol. B-Biol. 155, 39–50. https://doi.org/10.1016/j.jphotobiol.2015.12.011.

Mallikarjuna, K., Sushma, N.J., Reddy, B.S., Narasimha, G., Raju, B. D.P., 2013. Palladium nanoparticles: single-step plant-mediated green chemical procedure using Piper betle leaves broth and their anti-fungal studies. Int. J. Chem. Anal. Sci. 4, 14–18. https://doi.org/10.1016/j.ijcas.2013.03.006.

Meena, A.K., Bansal, P., Kumar, S., Rao, M.M., Garg, V.K., 2010. Estimation of heavy metals in commonly used medicinal plants: a market basket survey. Environ. Monit. Assess. 170, 657–660. https://doi.org/10.1007/s10661-009-1264-3.

Méndez-Albores, A., González-Arellano, S.G., Reyes-Vidal, Y., Torres, J., Ţălu, Ş., Cercado, B., Trejo, G., 2017. Electrodeposited chrome/silver nanoparticle (Cr/AgNPs) composite coatings: characterization and antibacterial activity. J. Alloy. Compd. 710, 302–311. https://doi.org/10.1016/j.jallcom.2017.03.226.

Nakkala, J.R., Mata, R., Sadras, S.R., 2016. The antioxidant and catalytic activities of green synthesized gold nanoparticles from *Piper longum* fruit extract. Process Saf Environ. 100, 288–294. https://doi.org/10.1016/j.psep.2016.02.007.

Nasrollahzadeh, M., Sajadi, S.M., Maham, M., Ehsani, A., 2015. Facile and surfactant-free synthesis of Pd nanoparticles by the extract of the fruits of *Piper longum* and their catalytic performance for the Sonogashira coupling reaction in water under ligand-and copper–free conditions. RSC Adv. 5, 2562–2567. https://doi.org/10.1039/C4RA12875C.

Ovais, M., Khalil, A.T., Islam, N.U., Ahmad, I., Ayaz, M., Saravanan, M., Shinwari, Z.K., Mukherjee, S., 2018. Role of plant phytochemicals and microbial enzymes in biosynthesis of metallic nanoparticles. Appl. Microbiol. Biotechnol. 102, 6799–6814. https://doi.org/10.1007/s00253-018-9146-7.

Poitevin, E., 2012. Determination of calcium, copper, iron, magnesium, manganese, potassium, phosphorus, sodium, and zinc in fortified food products by microwave digestion and inductively coupled plasma-optical emission spectrometry: Single-laboratory validation and ring trial. J. AOAC Int. 95, 177–185. https://doi.org/10.5740/jaoacint.CS2011_14.

Rajan, R., Chandran, K., Harper, S.L., Yun, S.I., Kalaichelvan, P.T., 2015. Plant extract synthesized silver nanoparticles: an ongoing source of novel biocompatible materials. Ind. Crops Prod. 70, 356–373. https://doi.org/10.1016/j.indcrop.2015.03.015.

Reddy, A.S., Zhang, S., 2013. Polypharmacology: drug discovery for the future. Expert Rev. Clin. Pharmacol. 6, 41–47. https://doi.org/10.1586/ecp.12.74.

Reddy, N.J., Vali, D.N., Rani, M., Rani, S.S., 2014. Evaluation of antioxidant, antibacterial and cytotoxic effects of green synthesized silver nanoparticles by *Piper longum* fruit. Mater. Sci. Eng. C. 34, 115–122. https://doi.org/10.1016/j.msec.2013.08.039.

Salehi, B., Zakaria, Z.A., Gyawali, R., Ibrahim, S.A., Rajkovic, J., Shinwari, Z.K., Khan, T., Sharifi-Rad, J., Ozleyen, A., Turkdonmez, E., Valussi, M., Tumer, T.B., Fidalgo, L.M., Martorell, M., Setzer, W.N., 2019. Piper species: a comprehensive review on their phytochemistry, biological activities and applications. Molecules. 24, 1364 https://www.mdpi.com/1420-3049/24/7/1364.

Scott, I.M., Jensen, H.R., Philogène, B.J., Arnason, J.T., 2008. A review of Piper spp. (Piperaceae) phytochemistry, insecticidal activity and mode of action. Phytochem. Rev. 7, 65–75. https://doi.org/10.1007/s11101-006-9058-5.

Silva-Ichante, M., Reyes-Vidal, Y., Bácame-Valenzuela, F.J., Ballesteros, J.C., Arciga, E., Ţălu, Ş., Méndez-Albores, A., Trejo, G., 2018. Electrodeposition of antibacterial Zn-Cu/silver nanoparticle (AgNP) composite coatings from an alkaline solution containing glycine and AgNPs. J. Electroanal. Chem. 823, 328–334. https://doi.org/10.1016/j.jelechem.2018.06.032.

Singh, J., Dutta, T., Kim, K.H., Rawat, M., Samddar, P., Kumar, P., 2018. Green synthesis of metals and their oxide nanoparticles: applications for environmental remediation. J. Nanobiotechnol. 16, 84. https://doi.org/10.1186/s12951-018-0408-4.

Ţălu, Ş., Stach, S., Méndez, A., Trejo, G., Ţălu, M., 2014. Multifractal characterization of nanostructure surfaces of electrodeposited Ni-P coatings. J. Electrochem. Soc. 161, D44–D47. https://doi.org/10.1149/2.039401jes.

Tripathi, D., Modi, A., Narayan, G., Rai, S.P., 2019. Green and cost effective synthesis of silver nanoparticles from endangered medicinal plant *Withania coagulans* and their potential biomedical properties. Mater. Sci. Eng. C. 100, 152–164. https://doi.org/10.1016/j.msec.2019.02.113.

Vidhu, V.K., Philip, D., 2014. Catalytic degradation of organic dyes using biosynthesized silver nanoparticles. Micron. 56, 54–62. https://doi.org/10.1016/j.micron.2013.10.006.

Yadav, R., Saini, H., Kumar, D., Pasi, S., Agrawal, V., 2019. Bioengineering of *Piper longum* L. extract mediated silver nanoparticles and their potential biomedical applications. Mater. Sci. Eng. C. 104,. https://doi.org/10.1016/j.msec.2019.109984 109984.

Zagoda, J.R., Porter, J.R., 2001. Aconveient microdilution method for screening natural products against bacteria and fungi. Pharm. Biol. 39, 221–225. https://doi.org/10.1076/phbi.39.3.221.5934.